Desalination and Water Treatment
www.deswater.com
doi: 10.1080/19443994.2013.773860

51 (2013) 6895–6904
November

Taylor & Francis
Taylor & Francis Group

Experimental study of high-performance hybrid NF-MSF desalination pilot test unit driven by renewable energy

Abdel Nasser A. Mabrouk[a,*], Hassan El-banna S. Fath[b]

[a]*Faculty of Petroleum & Mining Engineering, Department of Engineering Science, Suez University, Suez, Egypt*
Email: abdelnaser_mabrouk@s-petrol.suez.edu.eg
[b]*Faculty of Engineering, Department of Mechanical Engineering, Alexandria University, Alexandria, Egypt*

Received 23 September 2012; Accepted 2 February 2013

ABSTRACT

This study presents the experimental results of a renewable energy (RE) driven, high-performance multi-stage flash (MSF) desalination unit integrated with nanofiltration (NF) membrane. The desalination pilot test is built to evaluate, the performance of the novel De-aeration and brine Mix (MSF-DBM) configuration. The NF pilot is build in order to enable MSF desalination unit the operation at high top brine temperature (TBT). The capacity of the desalination pilot plant is 1.0 m^3/day of water. The whole pilot plant is installed at Wadi El-Natroun (Egypt). This study presents the first phase of the project, including the pilot test description, and experiments of concentrated solar trough, steam generator, NF and MSF units. Comparison between the simulation and the experimental results of the pilot unit' sub-systems are relatively satisfactory. The newly developed NF-MSF-DBM (de-aerator and brine mix) configuration is tested at TBT = 100 °C and the gain output ratio (GOR) is calculated as 15 which almost twice of traditional MSF under the same operating conditions. The newly high-performance NF-MSF-DBM and unit's input thermal energy which make the integration with (the relatively expensive) RE as a desalination plant driver is a viable option.

Keywords: Desalination; Renewable energy; MSF plant; NF membrane

1. Introduction

Desalination has been favored as a method to increase the water supply in many counties of the world. On the other hand, renewable energy (RE) as driver to desalination technologies is best suited to remote off-grid communities. Use of RE is more popular in academic circles and at test sites but has not been as popular with decision makers, who concentrate on large fossil-fueled desalination plant to provide potable water to large populations.

RE driven desalination systems fall into two categories. The first includes distillation processes driven by heat produced directly by the RE system (RES), while the second includes membrane and distillation processes driven by electricity or mechanical energy produced by RES. Attention has been directed toward improving the efficiencies of the solar energy conversions, desalination technologies, and their optimal coupling to make them economically viable for small- and medium-scale applications

Various small-scale RE desalination projects have been conducted in the Middle East and North Africa (MENA) region over the past twenty years. A hybrid

*Corresponding author.

multi-stage flash-reverse osmosis (MSF-RO) system driven by a dual purpose solar plant was installed in Kuwait, which produces 25 m^3 of water per day [1]. Pilot projects for solar pond collectors have been carried out in addition to multiple effect distillation (MED) desalination plant operated for 18 years at Umm El-Nar (Abu Dhabi) with a 120 m^3/day plant [1]. In Saudi Arabia, a PV-RO brackish water plant was installed and connected to a solar still with a production of 5 m^3/day [1]. These were small-scale projects that have contributed to the general consensus that renewable desalination is a feasible option in the Middle East. The most popular combination is either MED with thermal collectors or RO with photovoltaics (PV) technology.

The energy demand of seawater reverse osmosis (SWRO) plant located in Canary Islands, of a capacity of 25,000 m^3/d is provided by a combination of PV cells (rooftop) with minor share of the grid which consist of energy mix including wind energy [2].

There are various concentrated solar power (CSP) technologies. In 2011, 1.3 GW of CSP were operating and a further 2.3 GW were under construction [3]. Currently, base-load electricity generated by CSP plants costs two to three times that from existing fossil-based technologies without carbon capture and storage. CSP generation costs are competitive with photovoltaics and offshore wind but are almost two times of onshore wind [3]. A reduction of 50–60% in CSP generating cost, may reasonably expected over the next 10–15 years provided that research, development and demonstration programs are sustaining the commercial deployments of CSP plants. It is anticipated that CSP should become cost competitive with fossil-based load generation at some point between 2020 and 2030 [3].

The energy cost of solar desalination is reported as an equivalent to 5–15 kWh of electricity per cubic meter of water, either directly by reverse osmosis or indirectly as pump losses and decreased efficiency in backpressure turbines [4].

Multi stage flash (MSF) technology has proven to be a mature thermal technology for large-scale capacity production with high-quality desalinated water especially for high severe feed water quality. However, at high top brine temperature (TBT), scale deposits of high seawater brine concentration presents a real problem in MSF/MED plants as it directly affect the heat transfer rates on the heating surface. At higher temperature greater than 120˚C, nonalkaline calcium sulfate ($CaSO_4$) precipitates if saturation limits are exceeded, due to the inverse solubility of these salts with temperature. Formation of alkaline scale ($CaCO_3$ & MgOH) can be controlled by lowering pH (acid additives) or by adding antiscalant. Nonalkaline (hard) scale (as $CaSO_4$) is only controlled, nowadays, by limiting TBT below 120˚C.

Increasing TBT with hard scale control can be carried out by; (1) introduce high-temperature antiscalant, (2) reducing hard scale ions to avoid it reaching saturation conditions. The first approach, currently, is under experimental evaluation to check antiscalant performance under different operating conditions before introducing to the market [5]. The second approach is considered, in the literature [6–12], through the use of nanofiltration (NF) membrane system for make-up feed water pretreatment.

The application of NF membrane in seawater desalination has recently gained significant attention in the desalination industry due to selective removal of divalent ions. NF is originally applied to reject electrolytes and obtain ultrapure water with high-volume flux at low operating pressure, because most membranes have either positive or negative charge due to their compositions.

Extensive experiments have been carried out on MSF pilot test unit with NF as pretreatment [6–9]. NF pressure was 24 bars and its recovery ratio ranged from 60 to 65%. Almost 90% of the total concentration of the sulfate and calcium ions is rejected with NF brine, while the MSF make-up entirely formed from NF permeate was below their solubility limits. This result indicated the possibility to operate the MSF plant safely and without any scaling problem at TBT at or higher than 130˚C.

A partial pretreatment of the MSF feed (25% of make-up) by introducing NF membrane was proposed and presented in [10,11]. A test has been carried out on one evaporator of Layyah MSF plant located in UAE. The results showed an increase in the TBT from 105 to 110˚C and the production from 1,044 to 1,253 t/h (19.9%). The maximum production was 1,260 t/h (20.6%) at 117˚C with product conductivity of 454 μS/cm. However, based on personal communication, the NF plant was shut down due to operational problems in the pretreatment section.

The NF membrane possesses molecular weight cutoff of about hundreds to a few thousands, which is intermediate between RO membranes and ultrafiltration (UF). The pore radii and fixed charge density of practical membranes were evaluated from permeation experiments of different neutral solutes of sodium chloride. The pore radii of these NF membranes were estimated to range from 0.4 to 0.8 nm [12].

Simulation of a novel integrating NF system with MSF-de-aerator and brine mix (DBM) desalination plant at the TBT = 130˚C was carried out [13]. The process calculations showed that the gain output ratio

(GOR) of the novel configuration is tow times of the convention MSF-BR [13]. The levelized water cost of NF-MSF-DM (at TBT = 130˚C) was found to be 14% lower than conventional MSF (at 110˚C) at the current oil price of 104 $/bbl [13]. The novel NF-MSF-DBM configuration significantly reduces the unit's input thermal energy cost which suits integration with (the relatively expensive) RE.

The objective of this work is to present the pilot test description and experimental performance results of CSP, steam generator, NF, and MSF units. The well-developed process design program (VDS) [13–16] is upgraded to consider the mathematical model of CSP and steam generator and used as a process design tool for MSF-DBM, NF, steam generator, and CSP units.The goal of MSF desalination pilot test unit is to verify the new concept of (DBM-MSF) at high TBT and high performance.

2. Pilot test unit CSP-NF-MSF-DBM overview

The process design and simulation for the test pilot is developed to prepare specifications of different components. Some units are manufactured by Egyptian contractor, while other are purchased from vendors. The site is prepared where civil work and foundation are constructed. The test pilot components are installed, assembled and finally individual commissioning for each component is carried out. The site is located at 'Wadi El-Natroun,' remote area, almost 150 km southwest of Alexandria city (Egypt). The site belongs to Alexandria University.

Fig. 1 shows the pilot test of solar energy and desalination units. The concentrated solar parabolic trough with thermal energy storage facility provides the necessary heating in order to generate required steam of the MSF desalination unit. The system is equipped also with a backup boiler for steam compensation. Solar PV and wind turbine (not appeared in Fig. 1) are installed and run separately. However, in this phase, diesel engine is used to provide the pumps electricity until finalize the match and synchronization between PV and wind turbine.

2.1. MSF desalination unit

The MSF pilot unit consists of 28 flashing chambers with 28 connected condensers as shown in Figs. 2a and b. The stages are arranged in double deck in order to reduce the foot print. There are four sets; each set consists of 7 stages. MSF chambers are equipped with glass windows for monitoring the flashing process. The shell material of MSF is fabricated from 2–mm-thick stainless steel 316 L. The flash chamber is 0.5 m length and 0.5 m width, while the height is 1.0 m. The condenser tube is 8 mm diameter and 6 m long and made of stainless steel (0.7 mm thick). The number of tubes is 2 per condenser and arranged in multipass inside 0.5 m shell length. The unit is manufactured in Egyptian and assembled at the project site.

The orifice opening area controlled using gate valve which is located between the flash chambers. The interstages valves controls the interstages flow rates to guarantee the brine flashing at each stage. The splash plate is designed just above of the inlet opening to reduce carry over. Demister is fixed near the vapour outlet vapor pipes to reject brine carry over before going to the condenser. The shells are insulated to minimize energy losses. In addition to the brine heater, different supporting systems are added including vacuum system and chemical injection systems. The vacuum system has control valves at each stage to adjust the venting rate of noncondensable gases (NCG) and the stage pressure.

The MSF is the main subsystem where distillation is produced using the flashing process. Different instrumentations are installed to measure and record the temperatures, pressures, and flow rates as shown in Fig. 1. In the heating section, steam input and output temperatures in addition to pressure and flow are

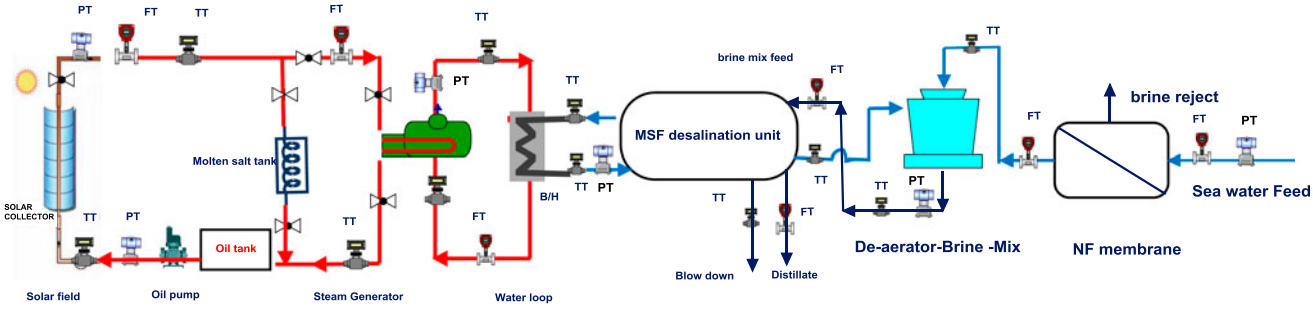

Fig. 1. Basic flow diagram of CSP-NF-MSF-DBM pilot plant.

(a) Photo of double deck MSF desalination test pilot unit

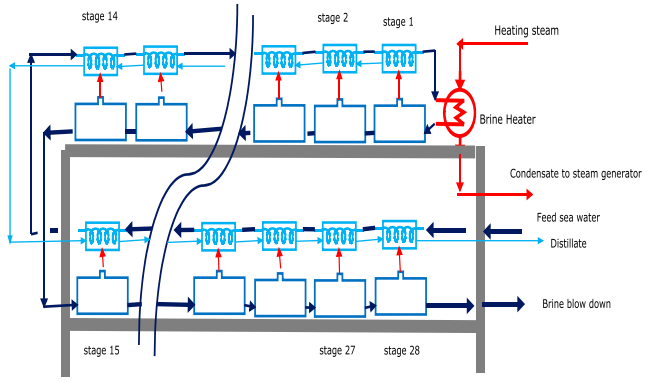

(b) Process flow diagram of Double deck MSF

Fig. 2. MSF desalination unit with double deck.

measured using proper transducers. All chambers are equipped with temperature and pressure indicators. First and last chambers are equipped with temperature transmitter (TT) and pressure transmitter (PT) and additional two movable PT and TT are supplied to be inserted in the chambers of the operator choice. Input seawater flow and output brine and distilled water flow rates are measured using flow transmitters.

2.2. Concentrated solar power (CSP) system

Four modules of solar concentrator (parabolic trough) are purchased and assembled in series at the site of the project as shown in Fig. 3. Each module is 3.6 m length and 1.524 m. width. The collector area per module is 5.6 m^2, while the collector reflective area is 5 m^2. The assembled collector length becomes 14.6 m, while the total area is 22.4 m^2. The receiver absorptivity is 0.92, the mirror reflectivity is 0.91, while the receiver emittance is 0.23. The black-coated pipes are 1.0 in. diameter and placed in 2.0 in. diameter glass pipes to minimize convection losses. The concentrators have a tracking system and were placed East–West and facing south.

Fig. 3. Four modules of concentrated solar collector in series.

The CSP system contains a steam generator to supply the MSF brine heater with the required heating steam. Thermal oil is circulated through the collecting pipes, gains the solar thermal energy and flow through steam generator, and energy storage tank.

The steam generator consists of shell and tube and has a separate vapor header. The shell diameter is 10 in. and 2 m length. The hot oil passes through tubes, while the water flows through the shell. The tube length is 4 m and diameter is 6 mm; the number of tubes is 24 and arranged in 2 passes.

The CSP system instrumented with TT, flow meters (FT), and PT, as shown in Fig. 1, to monitor the temperatures, flow rates and pressure in both steam and oil loops.

2.3. NF pretreatment

Fig. 4(a) shows the P and I diagram of the NF system. The system consisting of a dual media filter, a cartridge filter, a high-pressure pump, chemical injection pumps, and NF membrane. One dual media filter vessel is installed with a specified feed flow rate of 1.5 and 3.5 ton/hr for back wash. The vessel contains

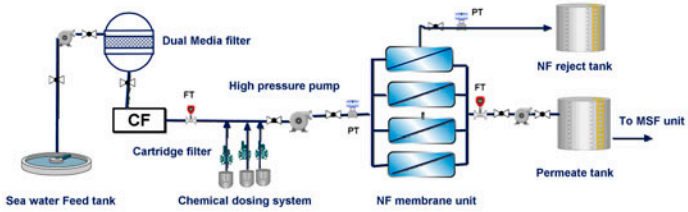

(a) Process Flow Diagram of NF system

(b) Photo of NF room

Fig. 4. NF system.

sand, gravel, and anthracite. The cartridge filter of 5 micron is installed after high-pressure pump and just before membrane section. The membrane section consists of 4 pressure vessels running in parallel each vessel contains one membrane element of NF270 4040 type. The whole NF system except feed, permeate, and brine tanks is placed inside one container with its control panel, as shown in Fig. 4(b). For the water salinity, samples are collected periodically to measure its conductivity using a mobile conductivity meter.

3. Pilot test performance

3.1. NF test performance

The NF system testing is carried out using the site brackish water (TDS = 2,000 ppm). On the other hand, a mathematical model of NF membrane is developed and verified against typical operating NF unit data using the Visual design and simulation (VDS) software developed by the authors [13–16]. The VDS simulation results of NF system at different feed pressure of 8 and 10 bar and compared with experimental results as shown in Table 1. The NF performance was carried out and assessed by the recovery ratio and salts rejection. The recovery ratio (permeate/feed) increases as the feed pressure increases. The salt rejection (1-(permeate salinity/feed salinity)) is calculated as shown in Table 1. The salt rejection decreases as the feed pressure increase due to increase in permeate salinity. The measured recovery ratio is slightly lower than the simulation results, although the salt rejection of experimental is lower than that of simulation. The difference between measured values of permeate flow, salinity, recovery ratio, salt rejection, and simulation results is within acceptable range.

3.2. Concentrated solar power (CSP) test performance

CPS system, including solar collector and steam generator, is simulated using VDS program. The mass and heat balance equations of solar collector, steam generator, and pumps are developed. The oil and water thermo physical properties correlations at different temperature are considered in the program. The characteristic surface of collector reflectivity, receiver emission and absorptivity, and glass tube material transmittance are specified in the VDS program. The specifications of the solar collector and steam generator are defined and fed to the program. The measured weather conditions (solar intensity, ambient temperature, and wind velocity) at each hour are fed to the program. The duration time starts at 7:00 AM to 8:00 PM with 1-hr step.

Fig. 5(a) shows the interface of VDS program results at 4:00 PM. The oil mass flow rate and temperature at inlet and outlet for both solar collector and the steam generator are presented. The collected energy is transferred to the steam generator to generate 3.8 kg/hr saturated steam at 113.8°C. The solar intensity (I) and calculated absorbed energy by the receiver is shown in Fig. 5(b). The difference is noticeable at mid-day time.

Fig. 6(a) shows comparison between the VDS simulation and experimental results of oil temperature rise through the solar collector along the day time. The oil temperature difference increases as the solar

Table 1
Typical NF pretreatment experimental results compared with VDS results

	VDS simulation	Experimental	% diff.	VDS simulation	Experimental	% diff.
Feed pressure, bar	8		–	10		–
Feed flow rate, ton/hr	1.325		–	1.375		–
Feed salinity, ppm	2000		–	2000		–
Permeate flow rate, ton/hr	0.67	0.6	−10	0.85	0.76	−11
Permeate salinity, ppm	648	600	−7	761	650	−15
Brine flow rate, ton/hr	0.65	0.725	12	0.52	0.6	15
Brine salinity, ppm	3,395	3,158	−7	4,027	3,760	−7
Recovery ratio %	51	45	−12	62	55	−11
Salt rejection, %	67.6	70	4	62	68	10

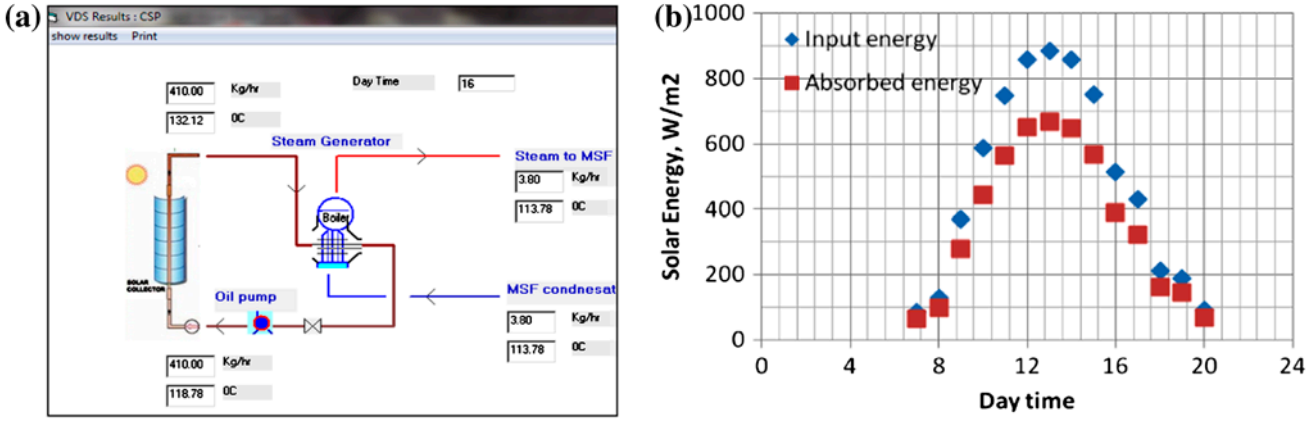

Fig. 5. (a) VDS simulation results of CSP system at 4:00 PM, June 2012 and (b) Measured solar intensity and absorbed energy by the receiver.

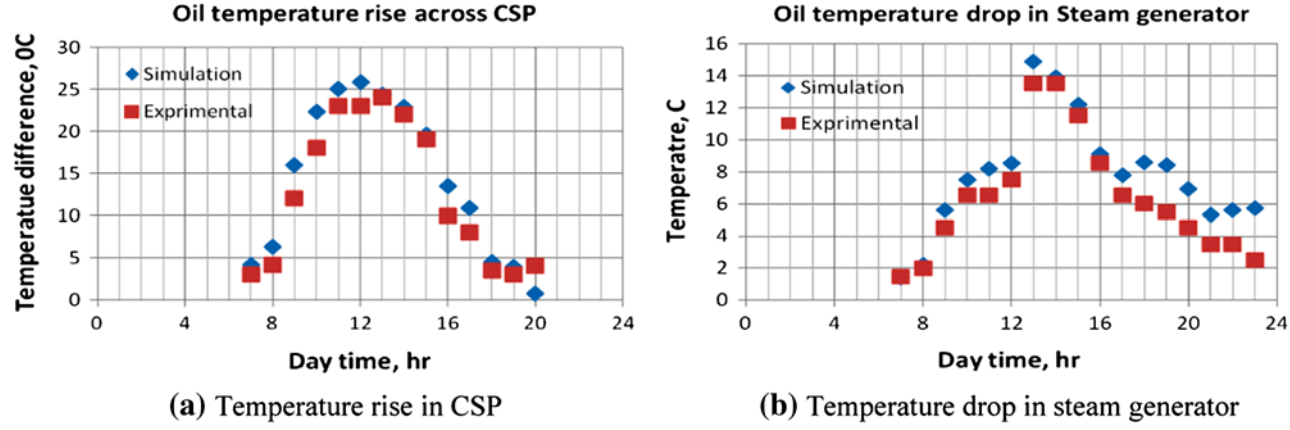

Fig. 6. Oil temperature variation through CSP trough & steam generator.

intensity increase, while the maximum difference in mid-day reach to 25˚C. Fig. 6(b) shows a comparison between the simulation and experimental results of the oil temperature drop in the steam generator unit. The maximum heat transfer occurs at the mid-day, and the maximum temperature drop is 14˚C. It is

noticed that at the same day time, the temperature drop in steam generator unit is less than the temperature rise in the solar collector. This means that part of gained energy in the collector is absorbed in the steam generator and the remaining is maintained with the outlet oil stream from steam generator and come back the collector. This explains the increase in oil temperature at the concentrated solar collector inlet through the day time.

The CSP system average efficiency (η_{CSP}) is calculated as the average useful gained power/average solar input power;

$$\eta_{CSP} = \frac{\dot{m}\, C_P\big|_{oil}(T_{o,oil} - T_{i,oil})}{I \times A_{CSP}} \quad (1)$$

Fig. 7 shows the simulation and experimental results of the collector efficiency through the day time. The collector efficiency decreases along the day time due to the increase in the average oil temperature, which increases the energy loss to the ambient. The experimental collector efficiency shows relatively low value than that of the simulation collector efficiency due to; (1) inaccurate tracking system that could not follow the sun movements accurately and (2) the inefficient concentrated tubes location in the CSP focus and possible convection loss.

Fig. 8 shows comparison between the simulated and the measured generated steam temperature. The water inlet and steam exit valve remain closed, while the oil valves are open to allow energy transfer from oil to heat the enclosed water in the boiler. The water feed and steam valves are opened when the water temperature reaches 77°C. The generated steam temperature increases as the solar intensity increase and the maximum temperature reached is 110°C at mid-day time.

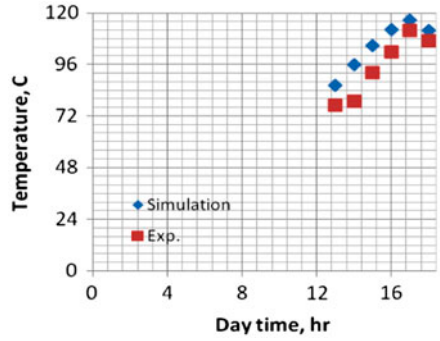

Fig. 8. Generated steam temperature.

The steam valve is opened at 1:00 PM at steam flow rate of 4.3 kg/hr. The generated steam is directed to MSF desalination unit as a heating source. The condensate steam in the brine heater of MSF is feed back to the steam generator. The amount of generated steam flow rate decreased linearly as shown in Fig. 9, this due to the decreasing in the solar collector efficiency. The measured generated steam flow rate shows lower values than the simulation results due to the thermal losses encountered through insufficient insulation of steam generator and throughout the connection pipe between CSP outlet and steam generator. As shown in Fig. 9, the operation of the steam generation extends up 11 PM this is due to heat storage in the CSP system.

Fig. 10 shows the simulation and experimental values of TBT variation through day time. As the CSP steam condenses in the brine heater of MSF, the TBT raise up due to gained energy of the latent heat. Under the ambient and operating condition of June 2012, the mid-day TBT reaches up to 100°C, while the CSP steam condenses at 106°C, that is, 6°C temperature differences is maintained.

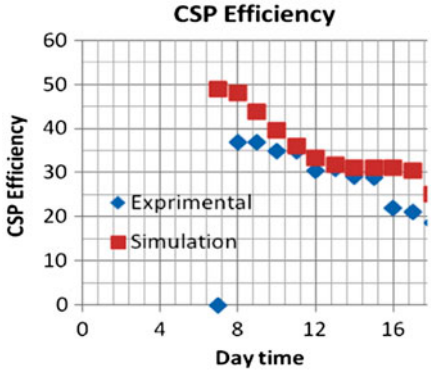

Fig. 7. Solar collector efficiency.

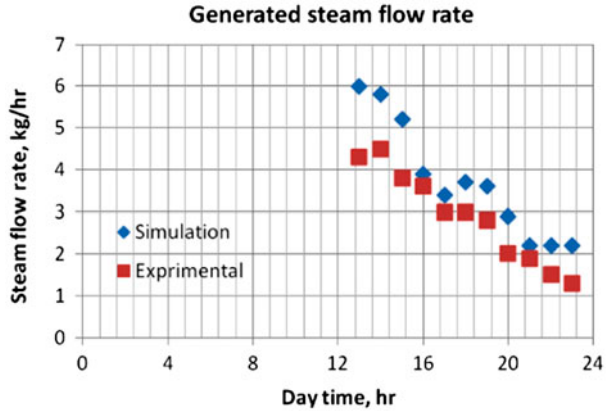

Fig. 9. Generated steam flow rate.

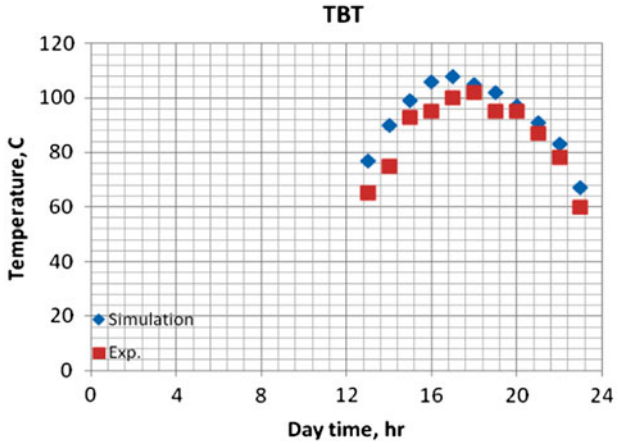

Fig. 10. TBT variation.

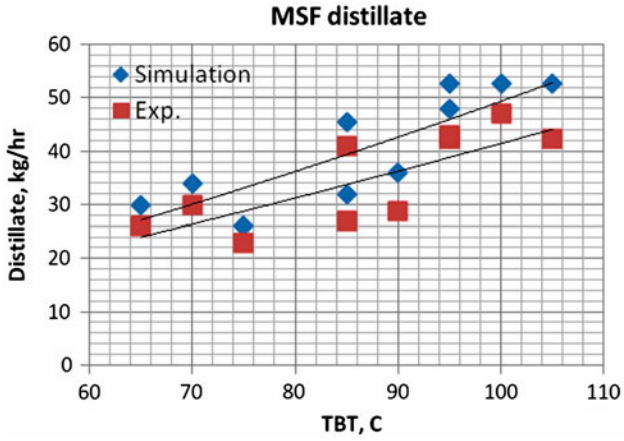

Fig. 11. MSF distillate productivity with TBT variation.

3.3. New MSF with De-aerator and Brine Mix (DBM)

The permeate water of NF system is directed to the deaeration and brine mix tower, where the feed is sprayed for oxygen removal. The deaerated water is mixed with part of the brine blow down then it pumped to the MSF condensers. The brine mix feed absorbs latent heat energy in condnesers before pass though brine heater where the brine reaches its TBT. The brine is then directed to the first flash chamber where flashing process occurs and vapor releases. The released vapor condenses to form a product water. The flashing process occurs in the successive stages until reach the last stage where the unflashed brine exit as brine blown down. The condensate of all stages is collected and directed to the water product tank. The brine level is adjusted above the interconnecting pipes (interstage gates) to guarantee the flash chambers sealing.

Under the same feed saline water flow rate (NF permeate) of 370 kg/hr and feed temperature of 27°C, and controlling the brine mix ratio at 20–70% of the MSF brine blow down, the distillate water is measured and recorded at different TBTs as shown in Fig. 11 as compared with design calculated values. The pressure of saline water before the first chamber is controlled and fixed value of 1.5 bar absolute (above saturation conditions) by partially closing the valve. Also the orifices among chambers are controlled by partially close the valve between each two successive chambers. The in tube water velocity is controlled at 2 m/s.

The rate of both the design and the measured distilled water increase as a result of TBT increases as shown in Fig. 11. The amount of distillate is lower than expected this may be due to the partial loss of flashed vapor through vacuum system and the irreversibility of flashing process occur within the orifices and weirs.

Fig. 12 shows the design and experimental GOR of MSF variation with TBT. This is defined as the ratio between distillate flow rate to the heating steam consumption, $\mathrm{GOR} = \frac{\dot{m}\ \text{distillate}}{\dot{m}\ \text{steam}}$. The average value of the unit design GOR is 17 which is almost twice the conventional MSF GOR. The average measured GOR is 15 as shown in Fig. 12. The small difference between the measured and designed value of GOR is due to the lower distillate productivity under fixed amount of heating steam flow rate.

The MSF specific power consumption (SPC) which is defined as the ratio between the pumping power consumption (kW) and the rate of water distillate (m^3/hr), $\mathrm{SPC} = \frac{\mathrm{PumpingPower}}{\dot{m}\ \text{distillate}}$. Fig. 13 shows that the SPC decreases as the TBT increase, mainly due to the increases in the water productivity. The experimental SPC is calculated based on the measured distillate flow rate and the rated power consumption. The

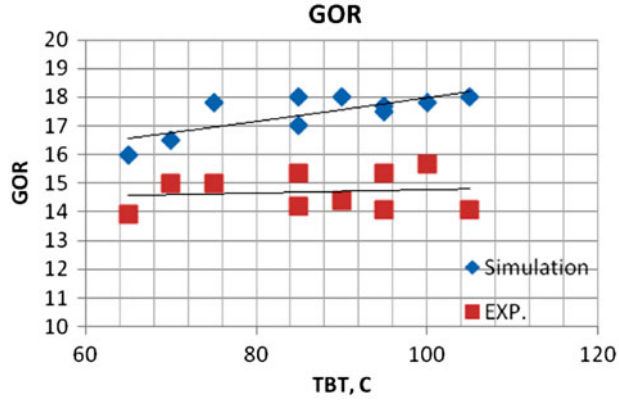

Fig. 12. The GOR of MSF system variation with TBT.

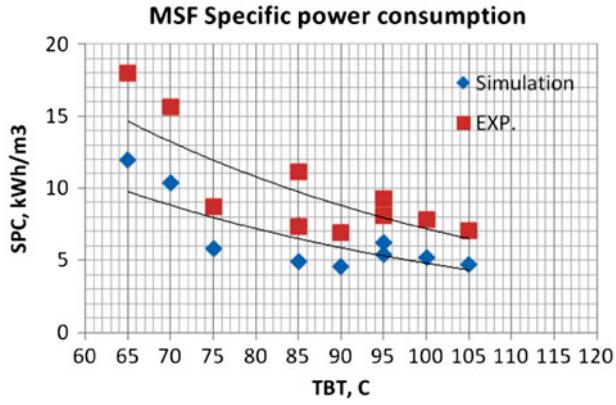

Fig. 13. SPC of MSF with TBT variation.

exprimental SPC is higher, however, than the design value is mainly due to lower experimental distillate for the same saline water feed and may be due to pressure drop in piping and valves that were not considered properly in the design stage. The SPC of test pilot unit is relatively higher than that of commercial value of large-scale MSF desalination plant due to the very small test pilot unit productivity.

In the next phase of the project, it is expected to run MSF system at TBT = 130˚C using heating steam at 140˚C from CSP system or auxiliary boiler for high TBT MSF. Completing insulation for all piping connected CSP and MSF and oil tank need to be finalized, proper operation of tracking system of CSP needed to be fix, also completing installation of the storage tank and filling with molten salt. Complete installation of back up boiler of 10 kg/hr capacity, in case of insufficient steam from CSP at high TBT requirements. Also matching and synchronize among PV and wind turbine electricity in 3 phases instead of 2 phase as per required for high-pressure pump of NF system and feed pump of MSF desalination unit.

4. Conclusion

- A pilot test unit of CSP-NF-MSF-DBM water desalination of 1.0 m^3/day capacity is designed and installed at Wadi AL-Natron, Egypt.
- The VDS [13–16] is upgraded to consider the mathematical model of CSP and steam generator and used as a process design tool for MSF-DBM, NF, steam generator and CSP units.
- Comparison between the numerical simulation and the experimental performance results of the pilot unit' subsystems are relatively satisfactory.
- The newly developed NF-MSF-DBM configuration is tested under TBT = 100˚C and the GOR is estimated as 15 which almost twice of traditional MSF under the same operating conditions.
- There is ongoing adjustment to operate the plant at TBT = 130˚C to improve the overall plant performance with expected GOR = 18.
- The newly high-performance NF-MSF-DBM desalination unit significantly reduces the unit's input thermal energy to suits integration with (the relatively expensive) RE as a desalination plant driver.

Acknowledgement

The authors acknowledge the financial support of research, development and innovation (RDI) program; project RE-NF-MSF (# C2-S1-148).

Nomenclature

A_{CSP}	—	area of solar collector, m^2
I	—	solar intensity, W/m^2
m	—	mass flow rate, kg/s
MSF	—	multistage flash
MED	—	multieffect distillation
RO	—	reverse osmosis
NF	—	nano filtration
CSP	—	concentrated solar power
TBT	—	top brine temperature, ˚C
GOR	—	gain output ratio
SPC	—	specific power consumption, kWh/m^3
Cp	—	specific heat capacity, kJ/kg k
TT	—	transmitter transducer
FT	—	flow meter transducer
PT	—	pressure transducer

References

[1] A. Fried, Water Industry Segment Report, World Trade Center, San Diego, 2011, www.wtcsd.org
[2] J.J. Sadhwani, J.M. Veza, Desalination and energy consumption in Canary Islands, Desalination 221 (2008) 143–150.
[3] The European Academies Science Advisory Council (EASAC) report, 2011, www.easac.eu.
[4] G. Fiorenza, V. Sharma, G. Braccio, Technoeconomic evaluation of a solar powered water desalination plant, Energy Conver. Manage. 44 (2003) 2217–2240.
[5] Amr Mahmoud, J. Robert, Abdelnasser Mabrouk, A. Imteyaz, A. Nafey, JS Choi, JK Park, S. Nied, J. Detering. New anti-scalant performance evaluation for MSF technology, Desalin. Water Treat. 1944-3994/1944-3986, 2012, http://dx.doi.org/10.1080/19443994.2012.704701
[6] O. Hamed, A. Hassan, K. Al-Shail, K. Bamardouf, S. Al-Sulami, Ali Hamza, M. Farooque, A. Al-Rubaian, Higher TBT, more product, less scaling, Desalin. Water Reuse, Vol. 13/3, IDA, Nov./Dec., 2003.
[7] A. Hassan, Fully Integrated NF-Thermal Seawater Desalination Process and Equipment, US Patents No. 2006/0157410 A1, July 20 (2006).

[8] M. Al Sofi, A. Hassan, G. Mustafa, A. Dalvi, N. Kithar, Nanofiltration as means of achieving higher TBT of >120 C in MSF, Desalination 118 (1998) 123–129.
[9] A. Hassan, M. Al Sofi, A. Al-Amoudi, A. Jamaluddin, A. Farooque, A. Rowaili, A. Dalvi, N. Kithar, G. Mustafa, I. Al-Tisan, A new approach to membrane and thermal seawater desalination processes using nanofilteration membranes (Part I), Desalination 118 (1998) 35–51.
[10] L. Awerbuch, Salt Water Desalination Process Using Ion Selective Membranes, International Patent (PCT), No. WO 01/14256 A1, March 1, 2001.
[11] L. Awerbuch, Water Desalination Process Using Ion Selective Membranes, US Patent No. 2005/0011832 A1, Jan. 20, 2005.
[12] X. Wang, T. Tsuru, M. Togoh, S. Nakao, S. Kimura, Evaluation of pore structure and electrical properties of nonfiltration membranes, J. Chem. Eng. Jpn. (1995) 186–192.
[13] Abdel Nasser Mabrouk, H. Fath. Techno-economic analysis of hybrid high performance MSF desalination plant with NF membrane, Desalin. Water Treat., 2012, http://dx.doi: 10.1080/19443994.2012.714893
[14] A.S. Nafey, H.E.S. Fath, A.A. Mabrouk, A new visual package for design and simulation of desalination processes, Desalination 194 (2006) 281–296.
[15] Abdel Nasser Mabrouk, A.S. Nafey, Hassan Fath, Steam, electricity and water evaluation of cogeneration power–desalination plants, Desalin. Water Treat. 22 (2010) 56–64.
[16] Abdel Nasser Mabrouk, Techno-economic Analysis of Seawater Desalination Plants. ISBN: 978-3-659-17934-1, LAP LAMBERT Academic Publishing, Germany, 2012.